

# Amoxicillin degradation with electro-persulfate combined with H<sub>2</sub>O<sub>2</sub> from aqueous solution using response surface methodology

Maryam Meserghani<sup>1</sup>, Mahnaz Nikaeen<sup>2</sup>, Ahmad Jonidi Jafari<sup>3</sup>, Mohammad Hadi Dehghani<sup>4</sup>, Bijan Bina<sup>2\*</sup>

<sup>1</sup>School of Public Health, Isfahan University of Medical Sciences, Isfahan, Iran

<sup>2</sup>Department of Environmental Health Engineering, School of Health, Isfahan University of Medical Sciences (IUMS), Isfahan, Iran

<sup>3</sup>Environmental and Occupational Hazards Control Research Center, Iran University of Medical Sciences, Tehran, Iran

<sup>4</sup>Department of Environmental Health Engineering, School of Public Health, Tehran University of Medical Sciences, Tehran, Iran

## Abstract

**Background:** Discharging wastewaters containing antibiotic into the environment causes some adverse effects on the human health and other organisms. The present study investigated the efficiency of electro-persulfate combined with hydrogen peroxide (H<sub>2</sub>O<sub>2</sub>) process as a chemical oxidation in amoxicillin (AMX) degradation.

**Methods:** Optimization of the significant operational independent variables was explored for removal of AMX. Central composite design (CCD) was employed as a statistical tool for experimental design. High-performance liquid chromatography (HPLC) was used for measuring AMX concentration. The most effective factors of the electro-persulfate and H<sub>2</sub>O<sub>2</sub> on the removal efficiency of AMX such as initial concentration of AMX, initial pH, PS/H<sub>2</sub>O<sub>2</sub> molar ratio, and the current density were measured.

**Results:** The optimum conditions for electro-persulfate removal efficiency of AMX to reach the degradation efficiency of higher than 95.28 ± 2.64% at reaction time of 60 minutes were obtained at pH = 4.23, AMX concentration = 31.9 mmol/L, current density = 39 mA/cm<sup>2</sup>, and PS/H<sub>2</sub>O<sub>2</sub> molar ratio = 0.82. AMX degradation was satisfactorily predicted by the quadratic model with high possibility and confidence level of 95%. The quadratic model had high regression coefficients (R<sup>2</sup> = 0.9964 and R<sup>2</sup><sub>adj</sub> = 0.9926), which was totally acceptable. The removal efficiency of AMX reduced from 87.3 ± 6.1 to 25.9 ± 9 as pH increased from 5.5 to 7.

**Conclusion:** According to the results, the electro-persulfate and H<sub>2</sub>O<sub>2</sub> process can be suggested as the most effective, high efficient, and in-situ chemical oxidation for degradation of AMX.

**Keywords:** Amoxicillin, Hydrogen peroxide, Oxidation-reduction, Antibiotic

**Citation:** Meserghani M, Nikaeen M, Jonidi Jafari A, Dehghani MH, Bina B. Amoxicillin degradation with electro-persulfate combined with H<sub>2</sub>O<sub>2</sub> from aqueous solution using response surface methodology. *Environmental Health Engineering and Management Journal* 2020; 7(3): 209–216. doi: 10.34172/EHEM.2020.24.

## Article History:

Received: 17 June 2019

Accepted: 19 September 2020

ePublished: 3 October 2020

## \*Correspondence to:

Bijan Bina

Email: [bbina123@yahoo.com](mailto:bbina123@yahoo.com)

## Introduction

Antibiotics have been a major parts of drugs used for treating infections and diseases since World War II (1,2). Amoxicillin (AMX) is one of the most commonly applied antibiotics in medicine. This drug belongs to a group of penicillins with semi-synthetic pattern and β-lactam ring (3). AMX takes antimicrobial activity against various microorganisms (4). The absorption of AMX in the human body is negligible and its major parts that are orally taken stay un-decomposed. This drug could be excreted through various methods such as feces and urine in different forms (metabolized and non-metabolized forms) (5,6). The pharmaceutical industry and hospital wastewater and

sewage treatment plant effluents contain high amounts of AMX due to their weak biodegradability. However, this antibiotic can be detected in other sources like agriculture, aquacultures, livestock, and slaughterhouses. The amount of AMX in these sources might be greater than the total amount of pharmaceutical agents (1,7). Some of the adverse effects caused by this drug include proliferation of antibiotic-resistant pathogens, gen-toxicity, accumulation in the environment, aquatic toxicity, and increasing chemical oxygen demand (8-10). Therefore, there are many concerns about adverse effects of these compounds on the public health and the environment because only a limited number of countries treat these wastewaters



before discharging into the environment (11-13). Thus, it is essential to employ a powerful and efficient technology for removing antibiotics from contaminated resources. A number of technologies have been taken for mineralization of AMX in the wastewater, include physicochemical processes such as electro-oxidation of AMX by sub-stoichiometric titanium oxide ( $Ti_4O_7$ ) (10), sonochemical degradation through sulfate radicals (9), UV/ $TiO_2$ , electrochemical degradation (12), magnetically modified graphene nano-platelets (14), UV and UV/ $H_2O_2$  (1), and UV/ $H_2O_2/TiO_2$  (7). Recently, electrochemical advanced oxidation processes (EAOPs) have been developed as promising technology for removal of contaminants from aqueous solutions (15,16). EAOPs include persulfate anions ( $E^0=2.6V$ ) and  $H_2O_2$  with activating agents such as electrochemical process ( $Fe^{2+}$  ion) that triggers the production of hydroxyl and other free radicals (17-19). This process has high removal efficiency and degrades the hazardous, refractory, and non-biodegradable organic pollutants from aqueous media (17,20,21). The advantages of in situ chemical oxidation include powerful and nonselective oxidation, widespread application (22,23), high efficiency, low energy costs, an extensive range of pH (2 to 10), and environmentally friendly process (18,24-26). The activation of peroxide and persulfate could be carried out with various techniques. The most common activation techniques are alkaline activation, electron transfer between transition metal ions, activated carbon, heat activation, and radiation (UV, visible light) (9,17,26). Similar to the Fenton reaction process, large amounts of free radicals could be generated during water electrolysis, which mainly occurs by the cathodic reduction. A large number of pollutants could be degraded by forming free radicals due to persulfate activation by  $Fe^{2+}$  (22,27). An advantage of the EAOPs is the rapid formation of divalent iron from the cathode reduction (17).

Radicals generated from sulfate also might be formed through other ways such as activation with electrolytic process (19,28,29). Several reactions and other chemical forms can influence the free radical equilibrium of chain reactions. Lifetime of hydroxyl radicals ( $2 \times 10^{-8}$  s) is shorter than that of sulfate radicals ( $3-4 \times 10^{-5}$  s). Thus, sulfate radicals can have a longer time for decomposing the pollutants (30). Peroxodisulfate and peroxymonosulfate can be utilized as an oxidant with persulfate with the potential of standard redox ( $E^0$ ) of 2.01 V and 1.82 V, respectively (31). Several studies have suggested persulfate and  $HO^\bullet$  radical or  $Fe^{2+}$  for degrading organic and inorganic compounds because of its high potential of standard redox (20,28,30). However, there is no study on the removal efficiency of AMX using electro-persulfate combined with  $H_2O_2$ . The aim of the present study was to find the optimum conditions for different effective factors (current density, initial pH, PS/ $H_2O_2$  ratio, and AMX concentration) by response surface methodology (RSM) for removal of AMX with the sulfate radicals/ $Fe^{2+}/H_2O_2$ .

## Materials and Methods

### Batch electrolysis experiments

The reactor ( $100 \times 100 \times 150$  mm) was made of plexiglass with 1.1 L capacity. Five iron electrodes with the same dimensions ( $100 \times 10 \times 5$  mm) were used in parallel mode. Iron plates were employed as the cathode and anode and the distance between the electrodes was 1 cm. A constant current for electrochemical reactor was provided using a direct current power supply. Figure 1 presents schematic diagram of reactor used in this study.

### Experimental procedures

An analytical grade of AMX and other chemicals including hydrogen peroxide ( $H_2O_2$ , 37%) and sodium persulfate ( $Na_2S_2O_8$ , 98%) was purchased from Sigma Aldrich (USA). A stock solution of AMX was prepared by dissolving certain amounts of AMX in deionized water, which was then diluted for the preparation of other samples. All experiments were carried out at  $25 \pm 1^\circ C$ . A certain volume of AMX stock solution and oxidants (HP and PS) was added into the batch reactor based on the experimental design. Persulfate and hydrogen peroxide with different ranges (0.5-0.75-1-1.25-1.75) were immediately added into the oxidation reactor before each run. Based on the ratio of persulfate and hydrogen peroxide, different dosages of  $Na_2S_2O_8/H_2O_2$  ranging (20/40, 40/50, 40/40, 50/40, 40/20 mmol/L) were added. Then, the electrical current was applied to start the degradation process. Agitation of the solution was done with a magnetic bar at 300 rpm for 60 minutes. Sodium hydroxide (NaOH) and sulfuric acid ( $H_2SO_4$ ) 1M was used for pH adjustment, and pH was measured by a pH meter (model: S-25). The samples were taken after 60 minutes. Then, the samples were filtered through a syringe filter ( $0.45 \mu m$ ) and added to a certain amount of methanol due to scavenging the remain of sulfate radical and kept until analysis of the concentration of residual AMX.

### Amoxicillin analysis

High-performance liquid chromatography (HPLC) was used for measuring AMX concentration. This HPLC

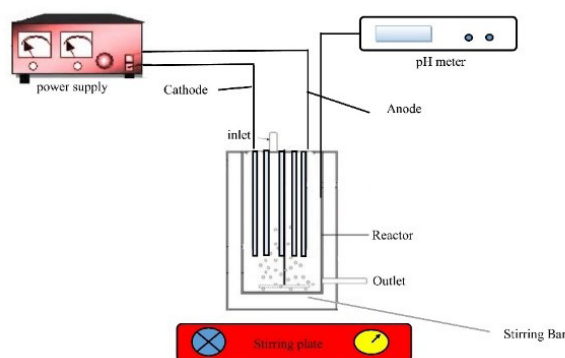


Figure 1. Schematic diagram of reactor used in the present study.

(Shimadzu UV-1600 spectrophotometer) comprised a Shimadzu LC-20 AB pump and a UV detector. A Shim-Pack VP-ODS-C18 column (dimensions: 250 mm × 4.6 mm, particle size: 5 μm) was employed for AMX analysis using chromatography apparatus. KH<sub>2</sub>PO<sub>4</sub> and acetonitrile solution with a ratio of 95:5 was used as a mobile phase with a flow rate of 1.0 mL/min, retention time of 5.5 minutes, and injection volume of 20 μL. The coefficient of calibration curve which was prepared with 8 standards, had a good linearity ( $R^2 = 0.999$ ).

### Experimental design

Optimization of the significant operating independent variables was explored for removal of AMX. Central composite design (CCD) was employed as a statistical tool for experimental design (25). The ranges of independent variables are shown in Table 1. The removal efficiency of AMX at reaction time of 60 minutes was measured as the response variable. According to Table 2, a total number of 28 experimental runs were designed which consisted 16 factorials, 6 axials, and 6 duplicates at the center point. Based on the results, all CCD experimental runs and interactions between parameters were analyzed using second-order polynomial model. The quadratic equation for the variables was as Eq. (1) (32,33):

$$Y = \beta_0 + \sum_{i=1}^k \beta_i x_i + \sum_{i=1}^k \beta_{ii} x_i^2 + \sum_{i=1}^{k-1} \sum_{j=2}^k \beta_{ij} x_i x_j + \dots + e \quad (1)$$

Where  $Y$  is the response predicted through the model (response variable or removal efficiency of AMX),  $\beta_0$  is the intercept (constant),  $x_i$  and  $x_j$  are the independent variables as coded values, the coefficient of  $e$  refers to the error of experiments and  $k$  is the number of factors studied,  $\beta_i$  represents the linear coefficient,  $\beta_{ii}$  is the quadratic coefficients, and  $\beta_{ij}$  is the interaction coefficients. The experimental design and data analysis were carried out using Design-Expert version 9.0.5 (Stat-Ease Inc., Minneapolis MN, USA). Analysis of variances (ANOVA) was done for analyzing the results. RSM was conducted to investigate the relationship between the results of observed and experimental variables as well as the interaction between different variables. All variables were considered at five levels, which are shown in Table 1. The  $\alpha$ -values could be designed using equation of  $\alpha = 2k/4$  (34,35).

### Results

In this study, the independent variables (current density, initial AMX concentration, initial pH, and persulfate/H<sub>2</sub>O<sub>2</sub> ratio) and dependent variable or response factor (AMX removal) were considered as the optimum operational conditions. The results showed that the current density of 30 mA/cm<sup>2</sup>, initial pH of 5.5, persulfate/hydrogen peroxide ratio of 1 could cause a high AMX removal. The reduced RSM models of the coded factors were determined to calculate AMX removal efficiency according to Eq. (2). Some variables in this model were not significant ( $P > 0.05$ ). Therefore, for better prediction ability, insignificant variables were removed from the model.

$$Y = 90.59 - 5.17 x_1 + 14.22 x_2 + 3.98 x_3 + 3.78 x_4 - 4.98 x_1 x_2 - 4.8 x_1^2 - 7.1 x_2^2 - 44.3 x_3^2 - 5.44 x_4^2 \quad (2)$$

Based on the coefficients in Eq. (2) which determine the effect of independent variables (current density, initial pH, and persulfate/H<sub>2</sub>O<sub>2</sub> ratio) on the AMX degradation, pH( $x_1$ ) had a negative effect on the response variable. It means that the degradation of AMX decreases with increasing pH level. However, the positive sign of other independent variables (current density and persulfate/H<sub>2</sub>O<sub>2</sub> ratio) indicates their direct effect on AMX degradation. Table 2 illustrates the experimental design and results of AMX removal efficiency. The results of ANOVA test obtained from the quadratic models for AMX degradation are presented in Table 3. The significance of model was also confirmed with the coefficient of the models ( $R^2 = 0.9964$ ). High  $R^2$  coefficient and low-value coefficient of variation (5.26%) present the admissible adaptation of the model for the experimental data. The adjusted purpose coefficient ( $R_{adj}^2 = 0.9926$ ) was close to the coefficient of the models ( $R^2 = 0.9964$ ), indicating that this model is trustable. The results of CV showed that only 5.26% of the variability in the degradation of AMX (response variable) was not described with the model. The insignificant lack-of-fit  $> 0.05$ , indicates that the quadratic model was fitted well with the predicted data. The ratio of adequate precision (42.35) ( $> 4$ ) illustrates the high precision and reliability of the model (36-38).

### Discussion

Based on the results, the normal probability plot is an

**Table 1.** Independent factors and coded levels according to the CCD

Variables	Unit	Symbols	Coded levels (xi)				
			- $\alpha$	-1	0	+1	+ $\alpha$
pH	-	X1	2.5	4	5.5	7	8.5
Current density	mA/cm <sup>2</sup>	X2	10	20	30	40	50
AMX concentration	mg/L	X3	10	20	30	40	50
PS/H <sub>2</sub> O <sub>2</sub> ratio	-	X4	0.5	0.75	1	1.25	2

**Table 2.** Experimental design and response variable for AMX degradation by CCD

Coded levels of variables				Removal efficiency (%)	
X1	X2	X3	X4	Observed	Predicted
4	40	20	0.75	39.45	35.22
5.5	30	30	1	87.75	90.59
5.5	30	30	1.5	72.18	70.02
5.5	10	30	1	32.16	33.75
2.5	30	30	1	82.83	81.73
7	40	40	1.25	45.05	40.78
7	20	20	0.75	12.15	6.78
4	40	40	1.25	66.24	61.08
5.5	30	30	0.5	68.23	61.27
4	20	40	0.75	19.21	25.08
5.5	30	30	1	94.16	90.59
5.5	30	30	1	92.72	90.59
7	20	40	0.75	15.18	14.74
7	40	20	1.25	35.56	42.78
7	40	40	0.75	34.39	33.12
5.5	30	30	1	92.35	90.59
7	20	40	1.25	23.25	22.3
4	20	20	0.75	18.06	17.12
5.5	30	30	1	93.36	90.59
7	20	20	1.25	18.25	14.34
8.5	30	30	1	65.24	62.05
4	40	40	0.75	55.36	53.12
5.5	30	30	1	94.04	90.59
7	40	20	0.75	24.87	23.26
4	20	20	1.25	19.34	14.72
5.5	50	30	1	94.26	97.27
4	20	40	1.25	24.98	22.68
4	40	20	1.25	57.91	53.12

appropriate graphical method for testing the normality of the residual. Figures 2 and 3 show the predicted vs actual data of AMX removal (%). The results of experiments were fitted well with the predicted data using the model. Thus, further data for validation of the model could be achieved. The graphical image as 2D contour plots or 3D response surface are a good option for demonstrating the interactive impact of effective variables on the removal efficiency of AMX. The effects of pH and current density on the removal efficiency of AMX are illustrated in Figure 4A and 4B. In these figures, the effect of interactions of pH and current density on the response variable (removal efficiency of AMX) is presented. Based on the results, the highest degradation of AMX ( $87.3 \pm 6.1\%$ ) was achieved at unadjusted pH of 5.5. Initial pH is a critical parameter which can influence the overall treatment efficiency (39). The performance of persulfate and  $H_2O_2$  depends on the solution pH because  $SO_4^{\cdot-}$  radical is dominant at low pH levels and  $HO^{\cdot}$  radical is predominant at high pH levels. This could describe that the removal efficiency of AMX reduces from  $87.3 \pm 6.1$  to  $25.9 \pm 9$  as pH increases from 5.5 to 7 and a slight increase in degradation was detected at pH = 8.5. Accordingly, most studies have considered persulfate as an activator. Generation of  $SO_4^{\cdot-}$  by the reduction of cathode electrode of persulfate anions could be accelerated at acidic pH. With increasing the amount of sulfate radical, AMX can be degraded during the process. So, pH plays an important role in all electro-activated persulfate oxidation process (27,39). It was found that one of the most significant parameters on the reaction rate of electrochemical systems is current density. Current

**Table 3.** The results of ANOVA for the reduced quadratic model for the removal efficiency of AMX

Source	Sun of squares	DF	Mean square	F-value	Prob>F	Remark
Model	2546.01	14	1819.14	259.30	0.0001	Significant
A-Ph	640.67	1	640.67	91.32	0.0001	Significant
B-CD	4854.71	1	4854.71	691.99	0.0001	Significant
C-AMX	253.45	1	253.45	36.13	0.0001	Significant
D-PS/ $H_2O_2$	343.53	1	343.53	48.97	0.0001	Significant
AB	396.41	1	396.41	56.50	0.0001	Significant
AC	11.19	1	11.19	1.59	0.2288	
AD	3.80	1	3.80	0.54	0.4747	
BC	33.64	1	33.64	4.80	0.0474	
BD	28.89	1	28.89	4.12	0.0634	
CD	0.036	1	0.036	5.146E-003	0.9439	
A <sup>2</sup>	561.15	1	561.15	79.99	< 0.0001	Significant
B <sup>2</sup>	1208.28	1	1208.28	172.23	< 0.0001	Significant
C <sup>2</sup>	11775.16	1	11775.16	1678.43	< 0.0001	Significant
D <sup>2</sup>	710.03	1	710.03	101.21	< 0.0001	Significant
Residual	91.20	13	7.02			
Lack of fit	76.91	8	9.61	3.36	0.0987	Not significant
Pure error	14.29	5	2.86			
Corrected total	2555.22	27				

R<sup>2</sup>= 0.9964, Adjusted R<sup>2</sup>= 0.9926  
Adequate precision= **42.353**  
C.V % = **5.26**

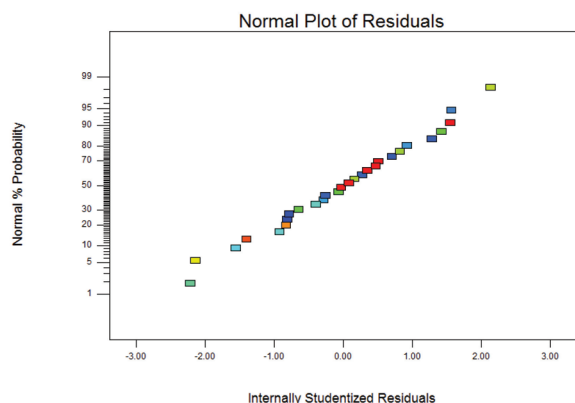
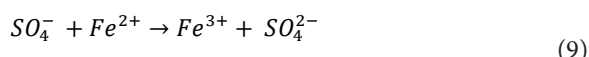
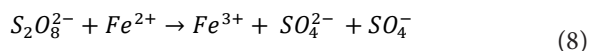
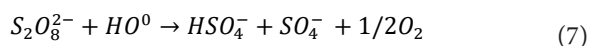
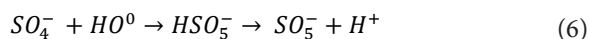
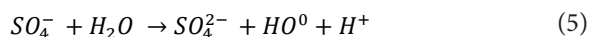


**Figure 2.** Plot of normal probability of the internally studentized residuals for AMX removal.

density could increase the generation of more sulfate radicals. In addition, more competition for adsorption of sulfate anions and  $O_2$  could create more sulfate radicals at higher electrode potentials. Therefore, sulfate radicals are mainly responsible for increasing removal efficiency. Current density in the range of 10-50 mA/cm<sup>2</sup> was studied in this study (Figure 4B). The increase in current density accelerates the production of free radicals such as hydroxyl and sulfate radical and even  $H_2O_2$ . Therefore, higher removal efficiencies of AMX can be achieved at higher loadings of  $Fe^{+2}$  (Eq. 2). The formation of iron ions ( $Fe^{+2}$ ) through chemical oxidation in anodic reduction activates persulfate (Eq. 8). Therefore, the reduction of cathode after being changed to  $Fe^{+3}$  based on Eq. (9). With further increase in the current density up to 40 mA/cm<sup>2</sup>, the degradation of AMX and rate constant slightly decreased, which is consistent with the results of previous studies (23,39). The generation reactions of sulfate and hydroxyl radicals activated by  $Fe^+$  are illustrated in Eqs. (2) to (9) (17,28,29).



The influence of AMX concentration and persulfate/ $H_2O_2$  ratio on the removal efficiency of AMX is presented in Figure 4C and 4D. Based on the results, the AMX removal was enhanced with increasing AMX concentration up to 30 mmol/L, and then, further increase in the AMX

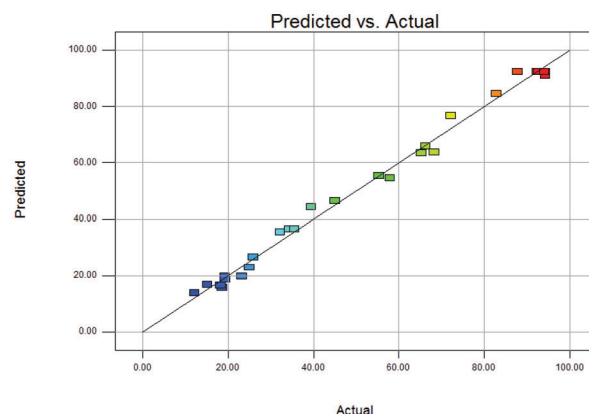


**Figure 3.** The response variables for experimental data versus predicted data in CCD for AMX removal.

concentration led to a decrease in the removal efficiency of AMX. To evaluate the performance of  $H_2O_2$  in enhancing persulfate oxidation, the ratios of persulfate to hydrogen peroxide were fixed to 0.5, 0.75, 1, 1.25, and 2 during 60 minutes of oxidation of AMX. The effect of persulfate/ $H_2O_2$  dosage on the removal of AMX was investigated in Figure 4B. Although persulfate reagent can act alone as an oxidant, if persulfate is activated by chemical or thermal methods, sulfate free radicals will be made, which are about 1000-10000 times stronger in destruction of organic pollutants (40).  $H_2O_2$  has been widely used to activate persulfate for degradation of pollutants (18). Increasing persulfate/ $H_2O_2$  ratio from 0.5 to 1 accelerated the degradation of AMX. Increasing the persulfate/ $H_2O_2$  ratio, and consequently, increasing the formation of sulfate and hydroxyl radicals improve degradation of AMX. Several studies have been reported this phenomenon for atrazine, tetracycline, 4-bromophenol, nitrobenzene, 2,4-dichlorophenoxyacetic acid (21,23,41).

## Conclusion

In this study, the efficiency of electro-persulfate combined with  $H_2O_2$  technique in removal of AMX was analyzed. RSM with CCD were adopted to determine the interaction of effective factors on the degradation of AMX, in order to determine the optimal parameters. The following results were obtained in the present study:

- The degradation of AMX was satisfactorily predicted according to the quadratic model because of high correlation coefficients ( $P < 0.05$ ).
- The quadratic model had high correlation coefficients ( $R^2 = 0.9964$  and  $R^2_{adj} = 0.9926$ ).
- The optimum conditions for degradation of AMX using electro-persulfate combined with  $H_2O_2$  were found at pH = 4.23, AMX concentration of 31.9 mmol/L, current density of 39 mA/cm<sup>2</sup>, and PS/ $H_2O_2$  molar ratio of 0.82, to reach the degradation of AMX higher than  $95.28\% \pm 2.64$  at reaction time of 60 minutes.

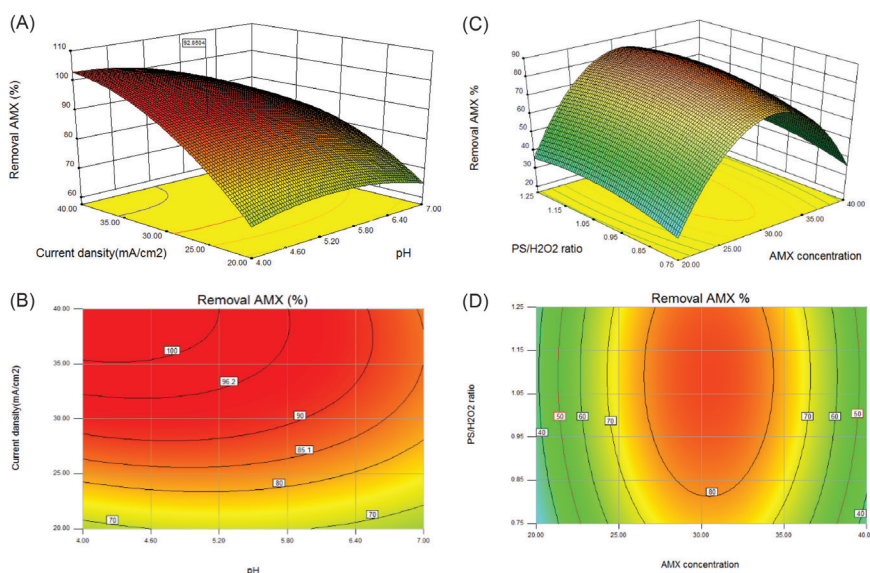


**Figure 4.** Plots of 2D contour and 3D response surface for the removal efficiency of AMX. (A and B): The effect of pH and current density on the removal of AMX; (C and D): The effect of current density and PS/H<sub>2</sub>O<sub>2</sub> ratio on the removal of AMX.

### Acknowledgments

The authors would like to gratitude the Research Department of Isfahan University of Medical Sciences for providing financial support for this study (Grant No: 397805) (Ethical code: IR.MUL.RESEARCH.REC.1398.054).

### Ethical issues

All authors certify that all data collected during the study are presented in this manuscript and no data from the study has been or will be published elsewhere separately.

### Competing interests

All authors declare that they have no conflict of interests.

### Authors' contributions

All authors have equally participated in all stages of the study including data collection, analysis, and interpretation, as well as the manuscript preparation.

### References

- Jung YJ, Kim WG, Yoon Y, Kang JW, Hong YM, Kim HW. Removal of amoxicillin by UV and UV/H<sub>2</sub>O<sub>2</sub> processes. *Sci Total Environ* 2012; 420: 160-7. doi: 10.1016/j.scitotenv.2011.12.011.
- Su S, Guo W, Yi C, Leng Y, Ma Z. Degradation of amoxicillin in aqueous solution using sulphate radicals under ultrasound irradiation. *Ultrason Sonochem* 2012; 19(3): 469-74. doi: 10.1016/j.ultsonch.2011.10.005.
- Homem V, Alves A, Santos L. Amoxicillin degradation at ppb levels by Fenton's oxidation using design of experiments. *Sci Total Environ* 2010; 408(24): 6272-80. doi: 10.1016/j.scitotenv.2010.08.058.
- Nosuhi M, Nezamzadeh-Ejhieh A. Comprehensive study on the electrocatalytic effect of copper - doped nano-clinoptilolite towards amoxicillin at the modified carbon paste electrode - solution interface. *J Colloid Interface Sci* 2017; 497: 66-72. doi: 10.1016/j.jcis.2017.02.055.
- Prayitno, Kusuma Z, Yanuwadi B, Laksmono RW. Study of hospital wastewater characteristic in Malang city. *Int J Eng Sci* 2013; 2(2): 13-6.
- Shaykhi ZM, Zinatizadeh AA. Statistical modeling of photocatalytic degradation of synthetic amoxicillin wastewater (SAW) in an immobilized TiO<sub>2</sub> photocatalytic reactor using response surface methodology (RSM). *J Taiwan Inst Chem Eng* 2014; 45(4): 1717-26. doi: 10.1016/j.jtice.2013.12.024.
- Elmolla ES, Chaudhuri M. Photocatalytic degradation of amoxicillin, ampicillin and cloxacillin antibiotics in aqueous solution using UV/TiO<sub>2</sub> and UV/H<sub>2</sub>O<sub>2</sub>/TiO<sub>2</sub> photocatalysis. *Desalination* 2010; 252(1): 46-52. doi: 10.1016/j.desal.2009.11.003.
- Tahiri E, Benaabidate L, Nejari C, Benbrahim KF. Assessment of physicochemical and biological parameters of Al Ghassani hospital wastewaters, Fez - Morocco. *J Mater Environ Sci* 2012; 3(1): 115-20.
- Eslami A, Asadi A, Meserghani M, Bahrami H. Optimization of sonochemical degradation of amoxicillin by sulfate radicals in aqueous solution using response surface methodology (RSM). *J Mol Liq* 2016; 222: 739-44. doi: 10.1016/j.molliq.2016.07.096.
- Ganiyu SO, Oturan N, Raffy S, Cretin M, Esmilaire R, van Hullebusch E, et al. Sub-stoichiometric titanium oxide (Ti(4)O(7)) as a suitable ceramic anode for electrooxidation of organic pollutants: a case study of kinetics, mineralization and toxicity assessment of amoxicillin. *Water Res* 2016; 106: 171-82. doi: 10.1016/j.watres.2016.09.056.
- Verlicchi P, Galletti A, Petrovic M, Barceló D. Hospital effluents as a source of emerging pollutants: an overview of micropollutants and sustainable treatment options. *J Hydrol* 2010; 389(3-4): 416-28. doi: 10.1016/j.jhydrol.2010.06.005.
- Padilla-Robles BG, Alonso A, Martínez-Delgado SA,

- González-Brambila M, Jaúregui-Haza UJ, Ramírez-Muñoz J. Electrochemical degradation of amoxicillin in aqueous media. *Chem Eng Process* 2015; 94: 93-8. doi: 10.1016/j.ccep.2014.12.007.
13. Ahmadian M, Yosefi N, Toolabi A, Khanjani N, Rahimi-Keshari S, Fatehizadeh A. Adsorption of direct yellow 9 and acid orange 7 from aqueous solutions by modified pumice. *Asian J Chem* 2012; 24(7): 3094-8.
  14. Kerkez-Kuyumcu Ö, Bayazit ŞS, Salam MA. Antibiotic amoxicillin removal from aqueous solution using magnetically modified graphene nanoplatelets. *J Ind Eng Chem* 2016; 36: 198-205. doi: 10.1016/j.jiec.2016.01.040.
  15. Hilles AH, Abu Amr SS, Hussein RA, El-Sebaie OD, Arafa AI. Performance of combined sodium persulfate/H<sub>2</sub>O<sub>2</sub> based advanced oxidation process in stabilized landfill leachate treatment. *J Environ Manage* 2016; 166: 493-8. doi: 10.1016/j.jenvman.2015.10.051.
  16. Ahmadzadeh S, Dolatabadi M. Modeling and kinetics study of electrochemical peroxidation process for mineralization of bisphenol A; a new paradigm for groundwater treatment. *J Mol Liq* 2018; 254: 76-82. doi: 10.1016/j.molliq.2018.01.080.
  17. Devi P, Das U, Dalai AK. In-situ chemical oxidation: Principle and applications of peroxide and persulfate treatments in wastewater systems. *Sci Total Environ* 2016; 571: 643-57. doi: 10.1016/j.scitotenv.2016.07.032.
  18. Matzek LW, Carter KE. Activated persulfate for organic chemical degradation: a review. *Chemosphere* 2016; 151: 178-88. doi: 10.1016/j.chemosphere.2016.02.055.
  19. Chen WS, Huang CP. Mineralization of aniline in aqueous solution by electrochemical activation of persulfate. *Chemosphere* 2015; 125: 175-81. doi: 10.1016/j.chemosphere.2014.12.053.
  20. Zhang Y, Zhang J, Xiao Y, Chang VW, Lim TT. Kinetic and mechanistic investigation of azathioprine degradation in water by UV, UV/H<sub>2</sub>O<sub>2</sub> and UV/persulfate. *Chem Eng J* 2016; 302: 526-34. doi: 10.1016/j.cej.2016.05.085.
  21. Delavaran Shiraz A, Takdastan A, Borghei SM. Photo-Fenton like degradation of catechol using persulfate activated by UV and ferrous ions: Influencing operational parameters and feasibility studies. *J Mol Liq* 2018; 249: 463-9. doi: 10.1016/j.molliq.2017.11.045.
  22. Bolobajev J, Trapido M, Goi A. Improvement in iron activation ability of alachlor Fenton-like oxidation by ascorbic acid. *Chem Eng J* 2015; 281: 566-74. doi: 10.1016/j.cej.2015.06.115.
  23. Nasser S, Mahvi AH, Seyedsalehi M, Yaghmaeian K, Nabizadeh R, Alimohammadi M, et al. Degradation kinetics of tetracycline in aqueous solutions using peroxydisulfate activated by ultrasound irradiation: effect of radical scavenger and water matrix. *J Mol Liq* 2017; 241: 704-14. doi: 10.1016/j.molliq.2017.05.137.
  24. Cai C, Zhang Z, Zhang H. Electro-assisted heterogeneous activation of persulfate by Fe/SBA-15 for the degradation of Orange II. *J Hazard Mater* 2016; 313: 209-18. doi: 10.1016/j.jhazmat.2016.04.007.
  25. Cruz-González K, Torres-Lopez O, García-León AM, Brillas E, Hernández-Ramírez A, Peralta-Hernández JM. Optimization of electro-Fenton/BDD process for decolorization of a model azo dye wastewater by means of response surface methodology. *Desalination* 2012; 286: 63-8. doi: 10.1016/j.desal.2011.11.005.
  26. Li Y, Yuan X, Wu Z, Wang H, Xiao Z, Wu Y, et al. Enhancing the sludge dewaterability by electrolysis/electrocoagulation combined with zero-valent iron activated persulfate process. *Chem Eng J* 2016; 303: 636-45. doi: 10.1016/j.cej.2016.06.041.
  27. Malakootian M, Yousefi N, Fatehizadeh A, Van Ginkel S, Ghorbani M, Rahimi S, et al. Nickel (II) removal from industrial plating effluent by Fenton process. *Environ Eng Manag J* 2015; 14(4): 837-42. doi: 10.30638/eemj.2015.093.
  28. Liu H, Bruton TA, Li W, Buren JV, Prasse C, Doyle FM, et al. Oxidation of benzene by persulfate in the presence of Fe(III)- and Mn(IV)-containing oxides: stoichiometric efficiency and transformation products. *Environ Sci Technol* 2016; 50(2): 890-8. doi: 10.1021/acs.est.5b04815.
  29. Wu X, Gu X, Lu S, Xu M, Zang X, Miao Z, et al. Degradation of trichloroethylene in aqueous solution by persulfate activated with citric acid chelated ferrous ion. *Chem Eng J* 2014; 255: 585-92. doi: 10.1016/j.cej.2014.06.085.
  30. Ghanbari F, Moradi M, Gohari F. Degradation of 2,4,6-trichlorophenol in aqueous solutions using peroxymonosulfate/activated carbon/UV process via sulfate and hydroxyl radicals. *J Water Process Eng* 2016; 9: 22-8. doi: 10.1016/j.jwpe.2015.11.011.
  31. Yang Y, Pignatello JJ, Ma J, Mitch WA. Effect of matrix components on UV/H<sub>2</sub>O<sub>2</sub> and UV/S<sub>2</sub>O<sub>8</sub>(<sup>2-</sup>) advanced oxidation processes for trace organic degradation in reverse osmosis brines from municipal wastewater reuse facilities. *Water Res* 2016; 89: 192-200. doi: 10.1016/j.watres.2015.11.049.
  32. Xie Y, Chen L, Liu R. Oxidation of AOX and organic compounds in pharmaceutical wastewater in RSM-optimized-Fenton system. *Chemosphere* 2016; 155: 217-24. doi: 10.1016/j.chemosphere.2016.04.057.
  33. Yousefi N, Nabizadeh R, Nasser S, Khoobi M, Nazmara S, Mahvi AH. Decolorization of Direct Blue 71 solutions using tannic acid/polysulfone thin film nanofiltration composite membrane; preparation, optimization and characterization of anti-fouling. *Korean J Chem Eng* 2017; 34(8): 2342-53. doi: 10.1007/s11814-017-0127-9.
  34. Arslan A, Veli S, Bingöl D. Use of response surface methodology for pretreatment of hospital wastewater by O<sub>3</sub>/UV and O<sub>3</sub>/UV/H<sub>2</sub>O<sub>2</sub> processes. *Sep Purif Technol* 2014; 132: 561-7. doi: 10.1016/j.seppur.2014.05.036.
  35. Yousefi N, Nabizadeh R, Nasser S, Khoobi M, Nazmara S, Mahvi AH. Optimization of the synthesis and operational parameters for NOM removal with response surface methodology during nano-composite membrane filtration. *Water Sci Technol* 2018; 77(5-6): 1558-69. doi: 10.2166/wst.2018.037.
  36. Dehghani MH, Zarei A, Mesdaghinia A, Nabizadeh R, Alimohammadi M, Afsharnia M. Adsorption of Cr(VI) ions from aqueous systems using thermally sodium organo-bentonite biopolymer composite (TSOBC): response surface methodology, isotherm, kinetic and thermodynamic studies. *Desalin Water Treat* 2017; 85: 298-312. doi: 10.5004/dwt.2017.21306.
  37. Dehghani MH, Shariati Niasar Z, Mehrnia MR, Shayeghi M, Al-Ghouti MA, Heibati B, et al. Optimizing the removal of organophosphorus pesticide malathion from water using multi-walled carbon nanotubes. *Chem Eng J* 2017; 310(Pt

- 1): 22-32. doi: 10.1016/j.cej.2016.10.057.
38. Dehghani MH, Zarei A, Mesdaghinia A, Nabizadeh R, Alimohammadi M, Afsharnia M. Response surface modeling, isotherm, thermodynamic and optimization study of arsenic (V) removal from aqueous solutions using modified bentonite-chitosan (MBC). *Korean J Chem Eng* 2017; 34(3): 757-67. doi: 10.1007/s11814-016-0330-0.
39. Sandhwar VK, Prasad B. Comparative study of electrochemical oxidation and electrochemical Fenton processes for simultaneous degradation of phthalic and para-toluic acids from aqueous medium. *J Mol Liq* 2017; 243: 519-32. doi: 10.1016/j.molliq.2017.08.016.
40. Salehi H, Ebrahimi AA, Ehrampoush MH, Salmani MH, Fouladi Fard R, Jalili M, et al. Integration of photo-oxidation based on uv/persulfate and adsorption process for arsenic removal from aqueous solutions. *Groundwater for Sustainable Development* 2020; 10: 100338. doi: 10.1016/j.gsd.2020.100338
41. Zhou Y, Zhang L, Cheng Z. Removal of organic pollutants from aqueous solution using agricultural wastes: a review. *Journal of Molecular Liquids* 2015; 212: 739-62. doi: 10.1016/j.molliq.2015.10.023.